Journal of
Nanoscience and Nanotechnology

Vol. 9, 3828–3836, 2009

Characterization of Au-Rh/TiO_2 Bimetallic Nanocatalysts by CO and CH_3CN Adsorption: XPS, TEM and FTIR Measurements

János Kiss[1,*], Róbert Németh[1], Ákos Koós[2], and János Raskó[1]

[1] *Reaction Kinetics Research Laboratory, Chemical Research Center of the Hungarian Academy of Sciences and*
[2] *Institute of Solid State and Radiochemistry, University of Szeged, H-6701 Szeged, P.O. Box 168, Hungary*

On X-ray photoelectron spectra of the Au-Rh/TiO_2 catalysts the position of Au4f peak was practically unaffected by the presence of rhodium, the peak position of Rh3d, however, shifted to lower binding energy with the increase of gold content of the catalysts. Rh enrichment in the outer layers of the bimetallic crystallites was experienced. The bands due to Au^0-CO, Rh^0-CO and $(Rh^0)_2$-CO were observed on the IR spectra of bimetallic samples, no signs for Rh^+-$(CO)_2$ were detected on these catalysts. The band due to CH_3CN on Lewis acid centers shifted to lower wavenumbers with the increase of Rh content, which shows that the strength of Lewis acid sites weakens with the increase of Rh content of the catalysts. CH_3CN, on the other hand, dissociates producing $CN_{(a)}$ species even at this temperature. From the shift to higher wavenumbers of the band due to $CN_{(a)}$ the strengthening of the C—N bond with increasing Rh content has been established. The results were interpreted by electron donation from titania through gold to rhodium and by the higher particle size of bimetallic crystallites. The effects of catalyst composition, reaction temperature and composition of the reacting gas mixtures have been studied on the oxidation of CO in the presence of hydrogen (PROX process). The presence of both O_2 and H_2 reduced the surface concentration of CO adsorbed on metallic sites. Mass spectroscopic analysis of the gas phase showed that gaseous CO_2 formed in the highest amount in $CO+O_2$ mixture, the presence of H_2 suppressed the amount of CO_2 produced. This negative effect of hydrogen was the lowest on 1% Rh/TiO_2, the highest inhibition was observed on Au/TiO_2 systems.

Keywords: Au-Rh Bimetallic Nanocatalysts, CO Adsorption, XPS, TEM, FTIR.

RESEARCH ARTICLE

1. INTRODUCTION

Hydrogen produced by the catalytic transformations (steam reforming or partial oxidation) of natural gas or alcohols[1,2] always contains significant amount of CO together with H_2O, CO_2 and CH_4. Before using hydrogen the concentration of CO (cca. 5–15%) must be lowered to 1–100 ppm for the proper operation of fuel cell producing energy with low environmental impact.[3] The most powerful process for the removal of CO proved to be the preferential oxidation (PROX) and/or the methanation of CO. Among other catalytic formulations supported Au nanoparticles have been tentatively tested in the PROX reaction[4–7] based on the high activity of dispersed gold on certain metal oxides for the low temperature oxidation of CO.[8–10] The important role of a reducible support in the PROX reaction has been demonstrated.[9,11–14] Although Au nanoparticles on TiO_2 (as a reducible support) has been found to be one of the most active catalysts for low temperature CO oxidation,[9,14] little is known on the catalytic behavior of Au/TiO_2 catalyst in the PROX reaction.

Another approximation for overcoming the problem caused by the relatively high concentration of CO in the fuel cell is to find a CO-tolerant H_2 oxidation catalyst, which works as an anode catalyst that oxidizes CO while maintaining high activity for H_2 electro oxidation under 373 K. For this purpose Pt-Sn/C, Pt-Rh supported on MoO_3 and on TiO_2 (Ref. [15]) and γ-Al_2O_3-supported Au-Pt[16] bimetallic systems might be good candidates.

The main concern in the field of bimetallic catalysis is what happens if a mixture of two metals is deposited onto an inorganic oxide support forming thereby a highly dispersed catalyst.[11] Ponec[12] has listed some effects due to diminished particle size.

In this work attempts have been made to characterize the TiO_2-supported Au-Rh bimetallic nanocatalysts

*Author to whom correspondence should be addressed.

by the adsorptions of CO and acetonitrile (CH_3CN) (as probe molecules) to study the possible electronic interaction between the two metallic components and between the support and the metallic part of the catalysts in order to elucidate the possible catalytic performance of these catalysts in CO oxidation and in the preferential oxidation of CO in the presence of hydrogen.

2. EXPERIMENTAL DETAILS

TiO_2 was the product of Degussa (P25, 50 m^2/g). For the preparation of 1 w% Au/TiO_2 catalyst, the pH of the $HAuCl_4$ aqueous solution (Fluka AG) was adjusted to pH = 7.5 by adding droplets of 1 M NaOH solution, and the fine powder of the oxide support was suspended in this solution. The suspension was kept at 353 K for 1 hour during continuous stirring. The suspension was aged for 24 hours at room temperature and washed with distilled water repeatedly, dried at 353 K and then calcined in air at 573 K for 4 hours. 1 w% Rh/TiO_2 catalyst was prepared by impregnating TiO_2 with an aqueous solution of $RhCl_3 \times 3H_2O$ salt (Johnson Matthey, 99.99% metal basis) to yield 1 w% metal content. The bimetallic Au-Rh catalysts with three different compositions were produced by impregnating TiO_2 with the mixtures of calculated volumes of $HAuCl_4$ and $RhCl_3 \times 3\ H_2O$ solutions to yield 1 w% metal content; with the variation in the volumes of metal compounds solutions the atomic percent of the metals varied: 25, 50 and 75 atomic percent Au corresponded to 75, 50 and 25 atomic percent Rh. The impregnated powders were dried in air at 383 K for 3 h. CO (99.97%), and H_2 (99.999%) were the products of Linde. CH_3CN (99%, Reanal) was used.

For IR studies the catalysts powders were pressed onto a Ta-mesh (30 × 10 mm, 5 mg/cm^2). The mesh was fixed to the bottom of a conventional UHV sample manipulator. It was resistively heated and the temperature of the sample was measured by NiCr-Ni thermocouple spot-welded directly to the mesh. The pretreatments of the samples were performed in a stainless steel UV IR cell (base pressure 1.33×10^{-7} mbar): the sample was heated in 1.33 mbar H_2 up to 573 K and it was kept at this temperature for 1 hour, this was followed by degassing at the same temperature for 30 min and by cooling the sample to the temperature of the experiment.

Infrared spectra were recorded with a Genesis (Mattson) FTIR spectrometer with a wavenumber accuracy of ±4 cm^{-1}. Typically 136 scans were collected. The whole optical path was purged with CO_2- and H_2O-free air generated by a Balston 75-62 FT-IR purge gas generator. The spectrum of the pretreated sample (background spectrum) and the actual vapour spectrum were subtracted from the spectrum registered in the presence of gas or gas mixtures. All subtractions were taken without use of a scaling factor ($f = 1.000$).

Mass spectrometric analysis was performed with the help of a QMS 200 (Balzers) quadrupole mass-spectrometer. XP spectra were taken with a Kratos XSAM 800 instrument using non-monochromatic Mg Kα radiation ($h\nu = 1253.6$ eV). TEM images were taken by a Philips CM 20 electron microscope at 300 K. Approximately 1 mg of products were put on a TEM grid.

3. RESULTS AND DISCUSSION

3.1. XPS Measurements

After recording the X-ray photoelectron spectra of as-received samples in vacuum, the catalysts were reduced in the preparation chamber in H_2 for 1 hour then H_2 was evacuated at 573 K; this was followed by cooling down to room temperature and transporting of the samples to the measuring chamber for obtaining the XP spectra of the reduced catalysts. Finally, the catalysts were contacted with CO (0.133 mbar) at 300 K for 15 min in the preparation chamber and after the evacuation of CO at 300 K, the XP spectra were recorded again. The peak position of Rh3d observed on the XP spectra of as-received samples shifted to lower binding energy after reduction. No appreciable change in the position of Au4f peak was recorded on the spectra of the reduced Au-containing samples in comparison with the as-received catalysts.

The position of the Au4f peak did not change with the variation of Au:Rh ratio of the reduced catalysts (Fig. 1(A)). A continuous shift to the lower binding energy in the position of Rh3d peak of the reduced samples, however, can clearly be recognized (Fig. 1(B)) with the increase of the Au content of the catalysts. The changes of peak areas for Ti2p, Au4f and Rh3d of the reduced catalysts as a function of the catalyst composition are depicted on Figure 1(C). The peak area of Ti2p slightly increased with the increase of Rh content, while the peak areas of Au4f and Rh3d changed according to the nominal composition of the catalysts. Based on the peak area values corrected by the sensitivity factors the $Area_{Au}/(Area_{Au} + Area_{Rh})$ and $Area_{Rh}/(Area_{Au} + Area_{Rh})$ ratios were calculated (Table I). The data clearly show that the outer layers contain more Rh than it could be expected from the nominal (bulk) composition of the catalysts. We did not observe further changes neither in the peak positions, nor in the peak areas after CO adsorption and evacuation at 300 K.

Although the number of works on bimetallic nanocluster has significantly grown in the last decades, no generally accepted theory concerning the catalytic effects of bimetallic catalysts can be found in the literature. It turned out in the very early stage of the studies that the models built up for the non-supported bimetallic systems, such as rigid band model,[17] formation of alloy,[18–20] surface enrichment in the component with lower heat of sublimation,[21] "cherry model,"[22] coherent potential approximation,[19,20] ensemble and ligand effect[21–25] and electron transfer[26,27]

RESEARCH ARTICLE

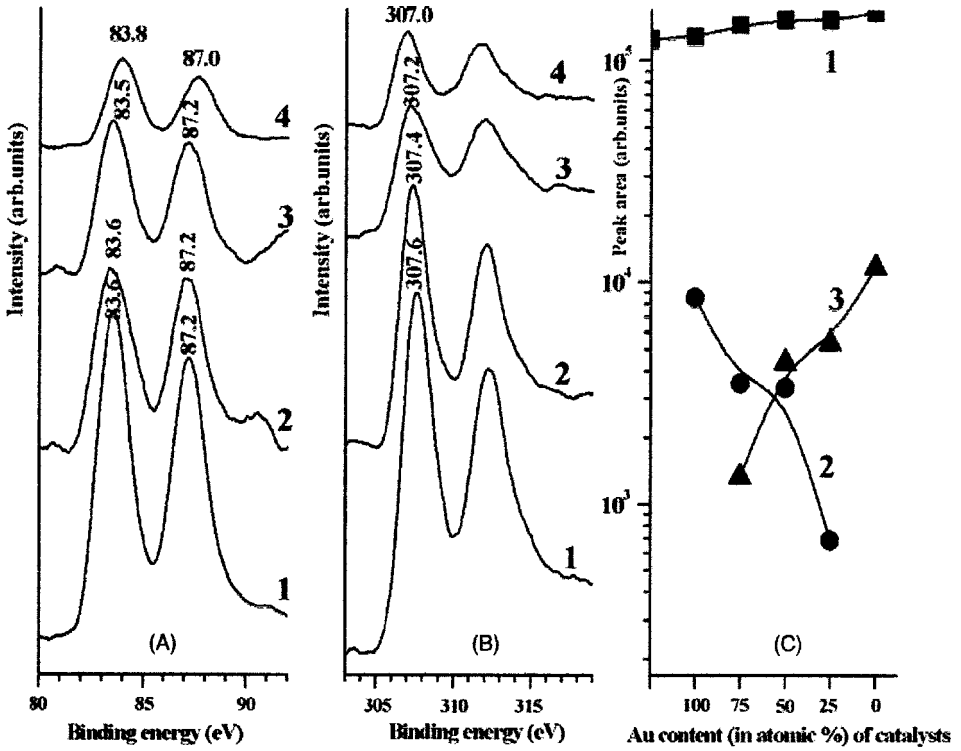

Fig. 1. (A)—Au4f region of XPS spectra of reduced catalysts: (B)—Rh3d region of XPS spectra of reduced catalysts (1—1% Rh/TiO_2; 2—1% (0.25Au + 0.75Rh)/TiO_2; 3—1% (0.5Au + 0.5Rh)/TiO_2 and 4—1% (0.75Au + 0.25Rh)/TiO_2) and (C)—XPS peak area of different components as a function of catalyst composition on the spectra of reduced catalysts (1—Ti2p; 2—Au4f and 3—Rh3d).

cannot be simply transformed to the supported bimetallic catalysts. UPS studies[28,29] revealed that metal crystallites having more than 150 atoms behave like a bulk metal. At lower particle sizes (*ca.* 50 metal atoms) the electronic structure is altered. Alloy formation can also be predictable in most cases of supported bimetallic systems, which can be influenced by the nature of the catalyst carrier.[30–33] The supporting oxide in our study was TiO_2, the reduction of which above 623 K would lead to strong metal support interaction (SMSI); this phenomenon may further strongly influence the electronic properties of the bimetallic particles. The reduction temperature (573 K) applied here hindered the occurrence of SMSI, thus this effect can be disregarded.

The present XPS results show that after the reduction of monometallic nanocluster, the corresponding metal is the peak position of Au4f was 83.6 eV, that of Rh3d was 307.6 eV on 1% Au/TiO_2 and 1% Rh/TiO_2, respectively. (The peak position of the bulk metals are: 83.7 eV (Au4f) and 307.0 eV (Rh3d) in our control experiments in harmony with the literature data[34]). With the increase of the Rh content the XPS peak position of Au4f remained practically constant (Fig. 1(A)), while that of Rh3d shifted to lower binding energy with the increase of Au content of the catalysts (Fig. 1(B)). The possible electron donation between the components of the catalysts is governed by the work function value ($\Delta\phi$) of the individual parts of the samples. The work function of reduced TiO_2 is 4.8 eV,[35] that for polycrystalline Au is 5.38 eV[36] and ($\Delta\phi$) of polycrystalline Rh is 4.98 eV.[37] On the basis of these literature data the most electron donating component should be TiO_2, the most electron accepting part of our catalysts has to be gold. According to the picture obtained in the present XPS study, however, Rh seems to be the most electron accepting component of the Au-Rh-TiO_2 nanosystem, as only its characteristic 3d peak shifted to lower binding energy with the increase of gold content. We suppose that the electron donation occurred from TiO_2 to gold and gold—in spite of the ($\Delta\phi$) values—conveyed the electrons to Rh. This is probably due to the filled d-orbital of gold and the difference in binding energy between Au4f and Rh3d orbitals.

The other effect for the binding energy shift of Rh3d is the change of the Rh size in the presence of Au. Increasing

Table I. Composition of the outer layers of the reduced catalysts based on XPS data.

Nominal composition	$Area_{Au}$/ ($Area_{Au} + Area_{Rh}$)	$Area_{Rh}$/ ($Area_{Au} + Area_{Rh}$)
1% Au/TiO_2	1.00	0.00
1% (0.75Au + 0.25Rh)/TiO_2	0.69	0.31
1% (0.50Au + 0.50Rh)/TiO_2	0.39	0.61
1% (0.25Au + 0.75Rh)/TiO_2	0.10	0.90
1% Rh/TiO_2	0.00	1.00

RESEARCH ARTICLE

the size, there are more screening electrons. As a consequence the core-hole screening is more effective and the binding energy of orbital shifts to lower energies.

3.2. TEM Study

In order to characterize and to estimate the sizes of different nanoclusters, TEM experiments were carried out. Using the preparation technique mentioned above the particle size of Au in monometallic 1% Au/TiO_2 is 6–7 nm. The size of Rh in 1% Rh/TiO_2 is somewhat higher then Au, it is measured around 7–8 nm. In the bimetallic nanosystem the metallic size has been changed. With increase of Rh content the metallic size increases. The size in the case of 1% (0.25Au + 0.75Rh)/TiO_2 measured to be 10–12 nm. These findings are consistent with the XPS results and confirm the FTIR results obtained during CO adsorption on these surfaces.

3.3. FTIR Analysis of CO Adsorption

Besides the 2180 cm^{-1} band (CO adsorbed on TiO_2), bands at 2130, 2094, 2051, 2026, 1968 and 1918 cm^{-1} appeared in the range of 2400–1800 cm^{-1} during the low pressure (0.0133 mbar–1.33 mbar) CO adsorption at 300 K on 1 w% Au/TiO_2 (Fig. 2(A)). With the increase of CO pressure to 1.33 mbar a shift from 2130 cm^{-1} to 2125 cm^{-1} was observed. In 13.3 mbar CO this band appeared at 2121 cm^{-1}. At the highest CO pressure applied here (13.3 mbar) one band with dramatically increased intensity at 2035 cm^{-1} appeared instead of the 2051 and 2026 cm^{-1} bands.

The adsorption of 0.0133 mbar CO on 1 w% Rh/TiO_2 caused the appearance of the bands at 2102, 2053, 1904 and 1858 cm^{-1} (Fig. 2(B)). With the increase of CO pressure the 2053 cm^{-1} band shifted to higher wavenumbers; in 13.3 mbar CO this band was observed at 2066 cm^{-1} and a new band at 1965 cm^{-1} appeared. Due to the evacuation at 300 K for 15 minutes the intensities of the bands slightly diminished and the band at 2066 cm^{-1} (observed in the presence of CO) shifted to 2055 cm^{-1}. The spectra due to CO adsorbed at 300 K on 1 w% (50 atomic% Au + 50 atomic% Rh)/TiO_2 sample illustrate what happened on the surfaces of bimetallic systems during CO adsorption (Fig. 2(C)). Bands due to CO adsorbed on Au-sites and on Rh-centers, respectively, can be distinguished even under the lowest CO pressure. The most striking change is observed in the position of the band around 2020 cm^{-1}, which belongs to an Au-CO species. This band appeared at 2012 cm^{-1} in 0.0133 mbar CO, its position shifted to higher wavenumbers with the increase of CO pressure. In 13.3 mbar CO it was observed at 2028 cm^{-1}. After a short evacuation at 300 K the intensity of all bands greatly reduced, the band that appeared at 2065 cm^{-1} in CO

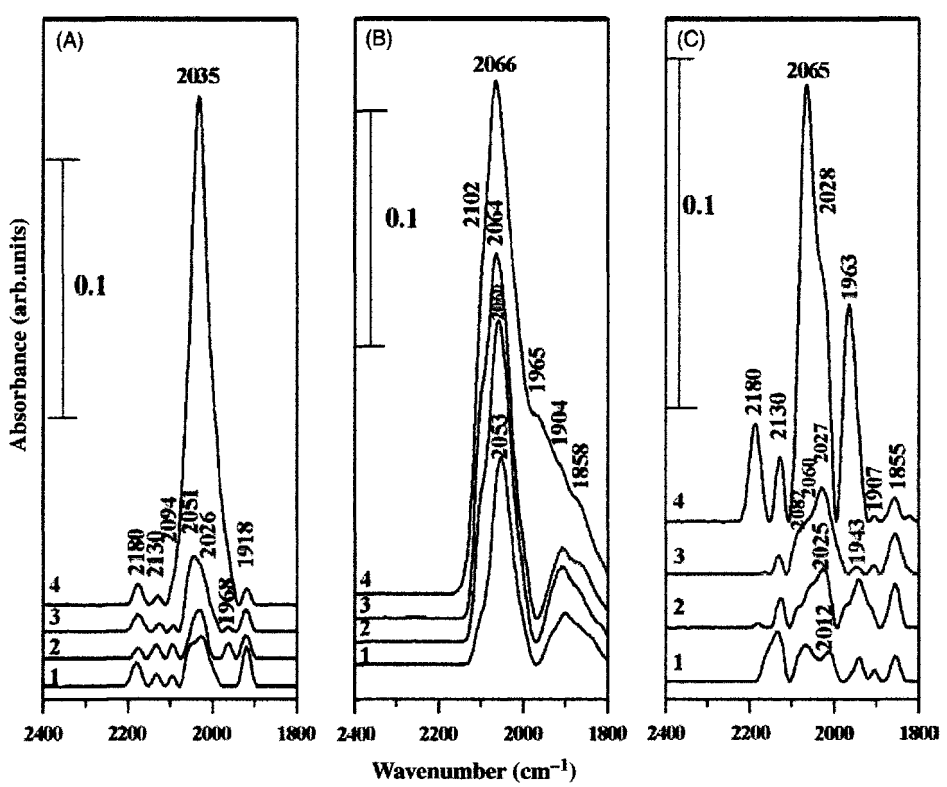

Fig. 2. IR spectra of reduced 1% Au/TiO_2 (A), 1% Rh/TiO_2 (B) and 1% (0.5Au + 0.5Rh)/TiO_2 (C) during CO adsorption at 300 K: 1—0.0133 mbar; 2—0.133 mbar; 3—1.33 mbar and 4—13.3 mbar. Adsorption time 15 min.

RESEARCH ARTICLE

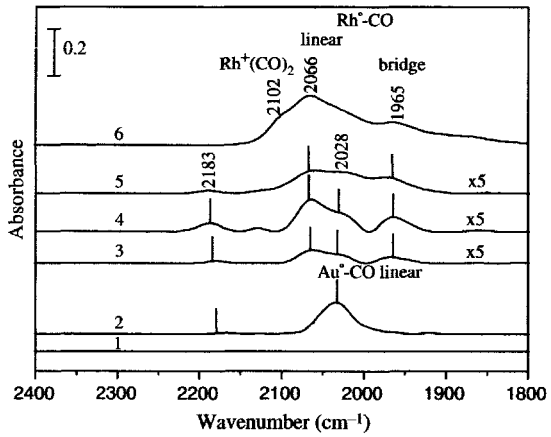

Fig. 3. IR spectra of reduced catalysts registered at 300 K in 13.3 mbar CO after 60 min adsorption time: 1—TiO_2; 2—1% Au/TiO_2; 3—1% (0.75Au + 0.25Rh)/TiO_2; 4—1% (0.5Au + 0.5Rh)/TiO_2; 5—1% (0.25Au + 0.75Rh)/TiO_2 and 6—1% Rh/TiO_2.

shifted to 2050 cm^{-1} and a new band at 2090 cm^{-1} (probably overlapped by the intense 2065 cm^{-1} band in CO) became clearly observable. Similar features were detected on other bimetallic nanoclusters, the intensity of the bands due to Rh-CO species evidently increased with the increase of Rh-content.

For proper comparison the spectra in 13.3 mbar CO after 60 minutes of adsorption at 300 K were depicted on Figure 3. It is to be noted that the adsorption capacity of the bimetallic systems was smaller than that of monometallic Au/TiO_2 and Rh/TiO_2 catalysts (see multiplication factors on the spectra of bimetallic catalysts). It can be noticed that bands due to Rh-CO species (2066, 1965 and 1860 cm^{-1}) were dominant on the spectra of bimetallic catalysts. CO uptake was the highest on monometallic catalysts (on 1% Au/TiO_2: 4.3 mg/gcat and on 1% Rh/TiO_2: 5.2 mg/gcat). The amounts of CO bonded to the surfaces of the bimetallic catalysts were substantially lower (1.1–3.1 mg/gcat). After the He- purge of the system at 300 K no CO desorption from Au/TiO_2 and bimetallic nanoclusters was observed in the TPD experiments.

From the experimental findings (Rh enrichment in the outer layers (Table I), lower capacity for CO adsorption of bimetallic catalysts) we intend to think that particles containing both Au and Rh atoms formed on the titania surface and the size of these bimetallic particles is greater than the particle size of monometallic catalysts. The intensity values of the bands due to adsorbed CO (Fig. 3) point out that the number of the adsorption sites greatly reduced by the presence of the second metal. Similarly to the former results[38–40] the band at 2066 cm^{-1} (CO adsorbed linearly to Rh^0) at 1965 cm^{-1} (bridged bonded CO, Rh_2^0CO) and at 2102 cm^{-1} (symmetric stretching of $Rh^+(CO)_2$) appeared on the spectrum of reduced 1% Rh/TiO_2. (This IR signal was detected when the crystallite size was very small.) Band due to the asymmetric stretching of $Rh^+(CO)_2$ around 2030 cm^{-1} was overlapped by the broad 2066 cm^{-1} band. In the cases of bimetallic Au-Rh samples, however, no signs for $Rh^+(CO)_2$ species (the presence of Rh^+ adsorption sites) were observed on the IR spectra. This can be regarded as a further proof of the electron donation from gold to rhodium in the bimetallic particles, which keeps Rh in reduced state.

3.4. FTIR Study of Acetonitrile Adsorption

Besides the band at 2291–2296 cm^{-1} due to CH_3CN molecularly adsorbed on weak Lewis acid sites (Ti^{+3}) a band at 2275–2283 cm^{-1} attributed to physisorbed acetonitrile was observed on all spectra. The band at 2334 cm^{-1} due to CH_3CN adsorbed on very strong Lewis acid sites[41–43] was detected only on the spectrum of 1% Au/TiO_2 in 1.33 mbar CH_3CN. The band registered at 2186–2197 cm^{-1} can be attributed to the CN vibration of CH_3CN molecules coordinated linearly through the lone electron pair of the N atom on Ti^{+3} or on metallic sites. The appearance of the bands in the range of 2170–2000 cm^{-1} can be due to $CN_{(a)}$ formed in the dissociation of acetonitrile on Ti^{+3} or metallic sites in different surface environments.

The bands due to δ_{as} (CH_3) (1430–1464 cm^{-1}), δ_s (CH_3) (1354–1370 cm^{-1}) and ρ (CH_3) (1035–1053 cm^{-1}) of molecularly adsorbed CH_3CN can be clearly distinguished at lower wavenumbers.

A band at 1698–1733 cm^{-1} was registered on the surfaces investigated. The band observed at 1655 cm^{-1} on Pt (111)[42] and at 1755 cm^{-1} on Pd (111)[43] was attributed to η^2 (C,N) CH_3CN adsorbed species, and it was concluded that the above difference in the positions of the bands is the consequence of the different softening of CN stretching mode: it was softened slightly less on Pd (111) than on Pt (111). Based on the above results obtained on single crystal surfaces, the band at 1698–1733 cm^{-1} detected in our studies is assigned to η^2 (C,N) CH_3CN species formed on the surfaces studied here.

The IR features observed at 2864–2876 cm^{-1}, 2760–2782 cm^{-1} and 1112–1130 cm^{-1} can be attributed to adsorbed CH_3NH_2.[44–47] The formation of methylamine might be connected with the participation of titania OH groups in the surface reactions.

The appearance of the bands at 1637–1653 cm^{-1} (δ (H_2O), at 1565–1590 cm^{-1} and 1519–1547 cm^{-1} (possibly due to surface carbonates) is the result of the surface oxidation of acetonitrile by the active oxygen of titania.

We have found no direct correlations between the positions, nor the integrated absorbance values of the above bands and the changes in the composition of the samples.

Next the interactions of 1.33 mbar CH_3CN were investigated isothermally at 300, 373, 473 and 573 K for 60 minutes. In these experiments the IR spectra were taken at the

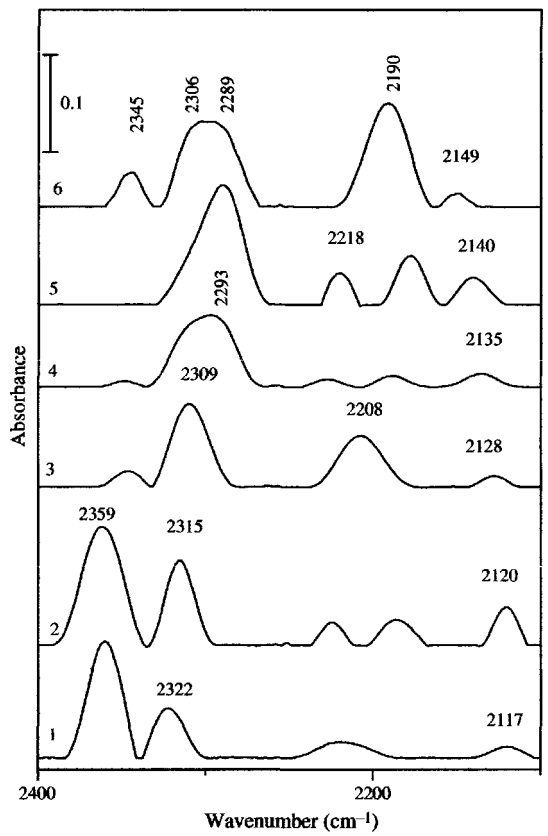

Fig. 4. 2400–2100 cm^{-1} region of the spectra registered in 13.3 mbar CH_3CN at 473 K after 60 min: 1—TiO_2; 2—1% Au/TiO_2; 3—1% (0.75Au + 0.25Rh)/TiO_2; 4—1% (0.5Au + 0.5Rh)/TiO_2; 5—1% (0.25Au + 0.75Rh)/TiO_2 and 6—1% Rh/TiO_2.

reaction temperature, and the spectra of the reduced catalyst and the gas phase were subtracted from the spectra registered in the reacting gas.

Differences in the C–N range of the IR spectra obtained in the CH_3CN adsorption on different nanosystems became more obvious at 473 K (Fig. 4). Bands at 2359 cm^{-1} (due to adsorbed CO_2), at 2322 cm^{-1} (CH_3CN adsorbed on very strong Lewis acid sites), at 2218 cm^{-1} (Ti-NCO) and at 2117 cm^{-1} ($CN_{(a)}$) appeared on the spectrum of TiO_2. On the spectrum of 1% Au/TiO_2 these bands were registered at 2359, 2315, 2218 and 2120 cm^{-1}. With the increase of the Rh content of the catalysts further continuous shift to lower wavenumbers occurred in the position of the band due to CH_3CN adsorbed on very strong Lewis acid sites; on catalysts having the highest amount Rh a band due to CH_3CN adsorbed on weak Lewis acid centres (2293–2289 cm^{-1}) also appeared. In our previous works a band attributed to acetonitrile coordinated on strong Lewis acid centres has been detected on both Au/TiO_2 (Ref. [45]) and Rh/TiO_2 catalysts.[44] On TiO_2 only the band due to actonitrile adsorbed on weak Lewis acid centres has been registered.[44–45] The formation of strong Lewis acid sites was connected with the presence of metals (Au and Rh), and it was interpreted as a consequence of the electron donation of Ti-cations on the surface to monometallic (Au and Rh) particles.

The shift observed here in the position of the band attributed to CH_3CN adsorbed on very strong Lewis acid sites with the increase of Rh content of the catalysts refers to the decrease in the electron withdrawing power Ti-cationic sites. The band due to $CN_{(a)}$ was shifted in the opposite direction: with the increase of Rh content this band shifted to higher wavenumbers. From these data it can be concluded that the increase of Rh content of the catalysts weakens the acid strength of Lewis centres, which is probably due to the less electron donation from titania to the metal particles. This would lead to the less electron back donation of metal particles to the antibonding orbital of the bond in $CN_{(a)}$, consequently the bond in $CN_{(a)}$ became stronger with increasing Rh content, thus the band due to $CN_{(a)}$ shifts to the higher wavenumbers.

3.5. PROX Reaction on Au-Rh/TiO_2 Bimetallic Nanocatalysts

The oxidation of CO in the presence of hydrogen (PROX process) was investigated on the above nanoclusters by mass spectrometric method. For comparison the experiments were performed by using of different gas mixtures. Among the MS data the intensity changes of gas phase CO_2 (as a measure of CO oxidation) on selected catalysts at 373 K were depicted on Figure 5. The highest amount of gaseous CO_2 was detected in $CO + O_2$ gas mixture on all samples. The data clearly show that the effectivity of monometallic Au/TiO_2 in CO oxidation is significantly suppressed by the presence of hydrogen; on 1% Rh/TiO_2 and on 1% (0.25Au + 0.75Rh)/TiO_2 catalysts, however, the negative effects were experienced only in the presence of higher amount of gaseous hydrogen. This finding can be interpreted on the basis of surface species detected during the above catalytic processes.

A detailed description of preferential CO oxidation on Au/TiO_2 has recently been given.[48] Similarly to the previous findings[5–7] CO adsorption proved to be weak on this sample. It was postulated that the increase of the reaction temperature, the presence of oxygen and hydrogen lowered the surface concentration of adsorbed CO. It was also suggested that Au/TiO_2 is not a suitable catalyst for preferential CO oxidation, as the amount of CO_2 (both in the adsorbed layer and in the gas phase) was highly suppressed by the presence of hydrogen. This was interpreted by the formation of formaldehyde.[48] Data obtained in the present work on 1% (0.75Au + 0.25Rh)/TiO_2 sample were similar in many respects to those experienced on 1% Au/TiO_2.

On the other monometallic catalyst (1% Rh/TiO_2) CO adsorbs in higher quantity than on 1% Au/TiO_2. In the $CO + O_2$ gas mixtures the intensities of the CO bands decreased, which shows that oxygen adsorption blocks a remarkable part of Rh sites at 300 K. At higher temperatures (323–373 K) the intensities of the bands due to

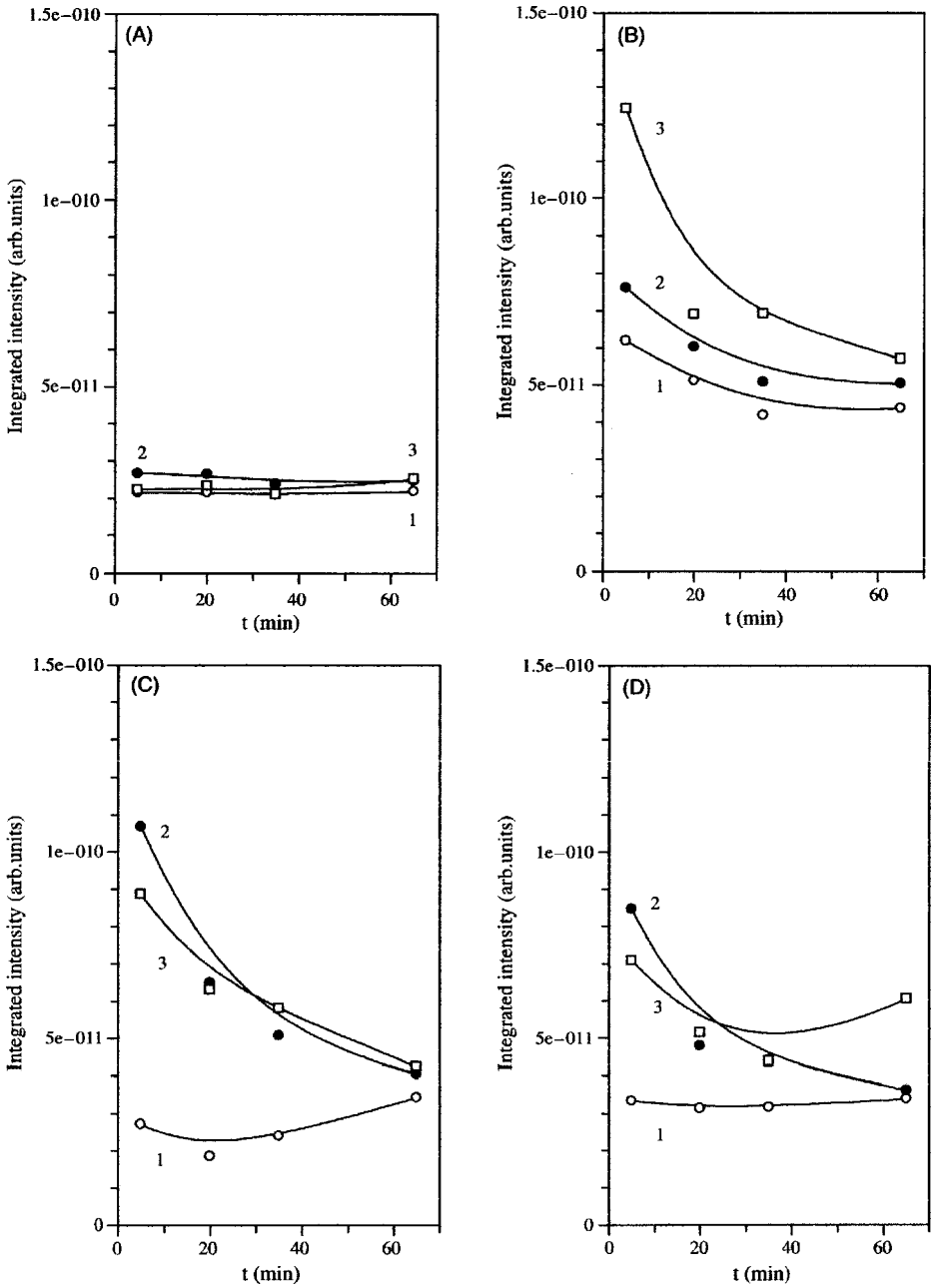

Fig. 5. Amounts of gaseous CO_2 (detected by MS) at 373 K in (A)—1.33 mbar CO; (B)—1.33 mbar CO + 0.133 mbar O_2; (C)—1.33 mbar CO + 0.133 mbar O_2 + 0.0133 mbar H_2 and (D)—1.33 mbar CO + 0.133 mbar O_2 + 0.133 mbar H_2 on: 1—1% Au/TiO_2; 2—1% (0.25Au + 0.75Rh)/TiO_2 and 3—1% Rh/TiO_2.

$Rh^+(CO)_2$ species increased and practically no IR features due to CO adsorbed on zerovalent Rh sites were observed in CO + O_2 mixtures. This is possibly due to the oxidation of Rh^0 centres to Rh^+ by gaseous oxygen. Addition of H_2 into the CO + O_2 mixtures caused a further dramatic decrease in the intensities of CO bands, which may be due to H_2 activation on the metallic sites. Thus a part of Rh surface sites may be occupied by H_2 dissociation reducing the number of active Rh sites in CO adsorption and its further oxidation.

The results obtained on 1% (0.5Au + 0.5Rh)/TiO_2 and on 1% (0.25Au + 0.75Rh)/TiO_2 samples were very similar to those observed on 1% Rh/TiO_2 catalysts. On the basis of the enrichment of Rh in the outer surface layers of bimetallic (Au-Rh) crystallites on TiO_2 (see above) it can be expected that the bimetallic Au-Rh catalysts show a CO adsorptive behavior similar to that observed on TiO_2-supported monometallic Rh sample.

Below 1800 cm^{-1} bands due to formate, bi- and monodentate carbonates and formaldehyde appeared on the

spectra. The formation of the above surface species was limited in CO alone on all catalysts, possibly due to the limited amount of surface active oxygen on TiO_2 surface. In the presence of oxygen and hydrogen, however, the intensities of the bands due to bi- and monodentate carbonates appreciably increased. Special attention has been paid to the formation of formaldehyde in the adsorbed layer. Recently it has been shown[48] that the formation of formaldehyde dramatically reduced the effectivity of PROX process on Au/TiO_2 catalyst. On the monometallic Rh/TiO_2 small intensity infrared bands for formaldehyde were detected in $CO + O_2 + H_2$ gas mixtures. On 1% $(0.75Au + 0.25Rh)/TiO_2$ bimetallic sample bands due to adsorbed formaldehyde were registered in all reacting gases at 300–373 K. The decrease of Au content in the bimetallic samples led to the disappearance of IR features assigned to $CH_2O_{(a)}$. On 1% $(0{,}25Au + 0.75Rh)/TiO_2$ these bands were missing in all reacting gas mixtures and at any temperatures. If we accept the former statement[48] that the formation of formaldehyde is disadvantageous in PROX process, its absence on 1% $(0.25Au + 0.75Rh)/TiO_2$ would make this sample a promising nanocomposit for the oxidation of CO in the presence of hydrogen.

4. CONCLUSIONS

(1) Electron donation from TiO_2 through Au to Rh occurs in TiO_2-supported bimetallic nanoclusters.
(2) Rh enrichment in the outer layers of bimetallic particles was observed.
(3) Adsorptive capacity of bimetallic catalysts was lower than that of monometallic samples, possibly due to the higher particle size in bimetallic crystallites.
(4) Acetonitrile bonds molecularly to the studied surfaces through lone pair electrons of its nitrogen to strong and weak Lewis acid sites of the support and through both carbon and nitrogen atoms of its CN (η^2 (C,N) species). Strength of Lewis acid sites weakens with the increase of Rh content of the catalysts.
(5) Acetonitrile dissociates producing $CN_{(a)}$. The bond strength of $CN_{(a)}$ becomes stronger with increasing Rh content of the catalysts.
(6) The interaction of gaseous CO with the lattice oxygen of titania leads to the formation of bi- and monodentate carbonates, bicarbonates and hydrocarbonate. The presence of H_2 in the gas phase increases the surface concentration of hydrocarbonate. All these surface species are spectators and are not involved in the surface reactions.
(7) The formation of adsorbed formaldehyde was also observed, which negatively affects he effectivity of the catalysts in CO oxidation.
(8) The surface concentration of CO adsorbed on metallic sites was reduced by the presence of both O_2 and H_2.
(9) The amount of gaseous CO_2 was suppressed by the presence of H_2 in the gas phase.
(10) Based upon the data on the formation of surface species and of gaseous products 1% $(0.25Au + 0.75Rh)/TiO_2$ sample seems to be a promising candidate among the Au-Rh bimetallic nanosystem for the oxidation of CO in the presence of H_2.

Acknowledgments: This work was financially supported by grants OTKA 46351, by the Hungarian National Office of Research and Technology (NKTH) and the Agency for Research Fund Management and Research Exploitation (KPI) under contract no. RET-07/2005 and by the Ministry of Education by NKFP 3A058-04 and NKFP OM-00411/2004. A loan of rhodium chloride from Johnson-Matthey is gratefully acknowledged.

References and Notes

1. J. N. Armor, *Appl. Catal.* 176, 159 (**1999**).
2. F. Aupretre, C. Descorme, and D. Duprez, *Catal. Commun.* 3, 263 (**2002**).
3. A. J. Appleby and F. R. Foulkes, Fuel Cell Handbook, Van Nostrand Reinhold, New York (**1989**).
4. G. Avgouropoulos, T. Ioannides, Ch. Papadopoulou, J. Battita, S. Hocevar, and H. K. Martalis, *Catal. Today* 75, 157 (**2002**).
5. G. K. Bethke and H. H. Kung, *Appl. Catal.* 194–198, 43 (**2000**).
6. M. J. Kahlich, H. Gasteiger, and R. J. Behm, *J. Catal.* 182, 430 (**2000**).
7. M. M. Schubert, M. J. Kahlich, H. Gasteiger, and R. J. Behm, *J. Power Sources* 84, 175 (**1999**).
8. M. Haruta, T. Kobayashi, S. Iijama, and F. Delannay, *Proc. 9th Int. Congr. Catal.* (**1988**), Vol. 3, p. 1206.
9. D. Cunningham, S. Tsubota, N. Kamijo, and M. Haruta, *Res. Chem. Intermed.* 19, 1 (**1993**).
10. M. A. Bollinger and M. A. Vannice, *Appl. Catal. B: Environmental* 8, 417 (**1996**).
11. A. Wootsch, C. Descorme, and D. Duprez, *J. Catal.* 225, 259 (**2004**).
12. O. Pozdnyakova, D. Teschner, A. Wootsch, J. Krönert, B. Steinhauer, H. Sauer, L. Tóth, F. C. Jenthoft, A. Knop-Gericke, Z. Paál, and R. Schlögl, *J. Catal.* 237, 1 (**2006**).
13. O. Pozdnyakova, D. Teschner, A. Wootsch, J. Krönert, B. Steinhauer, H. Sauer, L. Tóth, F. C. Jenthoft, A. Knop-Gericke, Z. Paál, and R. Schlögl, *J. Catal.* 237, 17 (**2006**).
14. S. Lin, M. A. Bollinger, and M. A. Vannice, *Catal. Lett.* 17, 245 (**1993**).
15. G. Avgouropoulus and T. Ioannides, *Appl. Catal. B* 56, 77 (**2005**).
16. S. Zhou, K. McIlwrath, G. Jackson, and B. Eichhorn, *J. Am. Chem. Soc.* 126, 1780 (**2006**).
17. D. A. Dowden and P. W. Reynolds, *Disc. Faraday Soc.* 8, 184 (**1950**).
18. D. F. Ollis, *J. Catal.* 23, 131 (**1971**).
19. W. H. M. Sachtler, Chemistry and Chemical Engineering of Catalysis Processes, edited by R. Prins and G. C. Schuit, Sijthoff and Noordhoff, The Netherlands (**1980**), p. 317.
20. V. Ponec and G. C. Bond (eds.), Catalysis by Alloys, Elsevier, Amsterdam (**1995**).
21. L. Guczi and A. Sárkány, Catalysis, Special Periodical Reports, edited by J. J. Spivey, The Society of Chemistry, London (**1994**), Vol. 11, p. 318, Chap. 8.
22. W. H. M. Sachtler and R. A. van Santen, *Adv. Catal.* 26, 69 (**1977**).
23. W. H. M. Sachtler and R. A. van Santen, *Appl. Surf. Sci.* 3, 121 (**1979**).
24. J. H. Sinfelt, *Acc. Chem. Res.* 10, 15 (**1977**).
25. J. K. A. Clarke, *Chem. Rev.* 75, 291 (**1975**).

26. V. Ponec, Electronic Structure and Reactivity of Solid Surfaces, edited by E. G. Derouane and A. A. Lucas, Plenum Press, New York **(1976)**, p. 537.
27. U. Bardi, A. Atrei, P. Ross, E. Zanazzi, and G. Rovida, *Surf. Sci.* 211–212, 441 **(1989)**.
28. J. W. He and D. W. Goodman, *J. Phys. Chem.* 94, 1502 **(1999)**.
29. R. C. Baetzold, *Surf. Sci.* 106, 243 **(1981)**.
30. R. C. Baetzold and J. Hamilton, Progress in Solid State Chemistry, Pergamon Press, New York **(1983)**, Vol. 15, p. 1.
31. N. Wagstaff and R. Prins, *J. Catal.* 59, 434 **(1979)**.
32. P. S. Kirlin, B. R. Strochmeier, and B. C. Gates, *J. Catal.* 98, 308 **(1986)**.
33. H. Topsoe, J. A. Dumesic, E. G. Derouane, B. S. Clause, S. Morup, J. Villadsen, and N. Topsoe, Preparation of Catalysts, edited by B. Delmon et al., Elsevier, Amsterdam **(1979)**, Vol. 2, p. 365.
34. C. D. Wagner, W. M. Riggs, L. E. Davis, J. F. Moulder, and G. E. Muilenberg, Handbook of X-ray Photoelectron Spectroscopy, Perkin-Elmer Co **(1978)**.
35. Y. W. Chung, W. Lo, and G. A. Somorjai, *Surf. Sci.* 64, 588 **(1977)**.
36. M. Uda, A. Nakamura, T. Yamamoto, and Y. Fujimoto, *J. Electr. Spectr.* 88–91, 643 **(1998)**.
37. CRC Handbook of Chemistry and Physics, CRC Press, Boca Raton FL **(1979)**.
38. F. Solymosi and M. Pásztor, *J. Phys. Chem.* 89, 4783 **(1985)**.
39. M. Primet, *J. Chem. Soc. Faraday Trans.* 74, 2570 **(1978)**.
40. C. A. Rice, S. D. Worley, C. W. Curtis, J. A. Guin, and A. R. Tarrer, *J. Chem. Phys.* 74, 6748 **(1981)**.
41. J. Raskó and J. Kiss, *Appl. Catal. A. General* 303, 56 **(2006)**.
42. J. Raskó and J. Kiss, *Catal. Lett.* 109, 71 **(2006)**.
43. J. Raskó and J. Kiss, *Appl. Catal. A. General* 298, 115 **(2006)**.
44. N. R. Avery, T. W. Matheson, and B. A. Sexton, *Appl. Surf. Sci.* 22–23, 384 **(1985)**.
45. K. Murphy, S. Azad, D. W. Bennett, and W. T. Tysoe, *Surf. Sci.* 467, 1 **(2000)**.
46. J. Gray and R. C. Lord, *J. Chem. Phys.* 26, 690 **(1957)**.
47. T. S. Nunney, J. J. Birtill, and R. Raval, *Surf. Sci.* 427–428, 282 **(1999)**.
48. J. Raskó and J. Kiss, *Catal. Lett.* 111, 87 **(2006)**.

Received: 28 June 2007. Accepted: 14 October 2007.